Electronic Supplementary Material (ESI) for Physical Chemistry Chemical Physics

Supplementary Information

Glucose Oxidase Nanotube-Based Enzymatic Biofuel Cells with Improved Laccase Biocathodes

Jihun Kim[a] and Kyung-Hwa Yoo[a*]

Department of Physics and National Core Research Center for Nanomedical Technology, Yonsei University, 134 Shinchon-dong, Seodaemun-gu, Seoul 120-749, Korea

*Corresponding author

E-mail address: khyoo@yonsei.ac.kr (K.-H. Yoo)

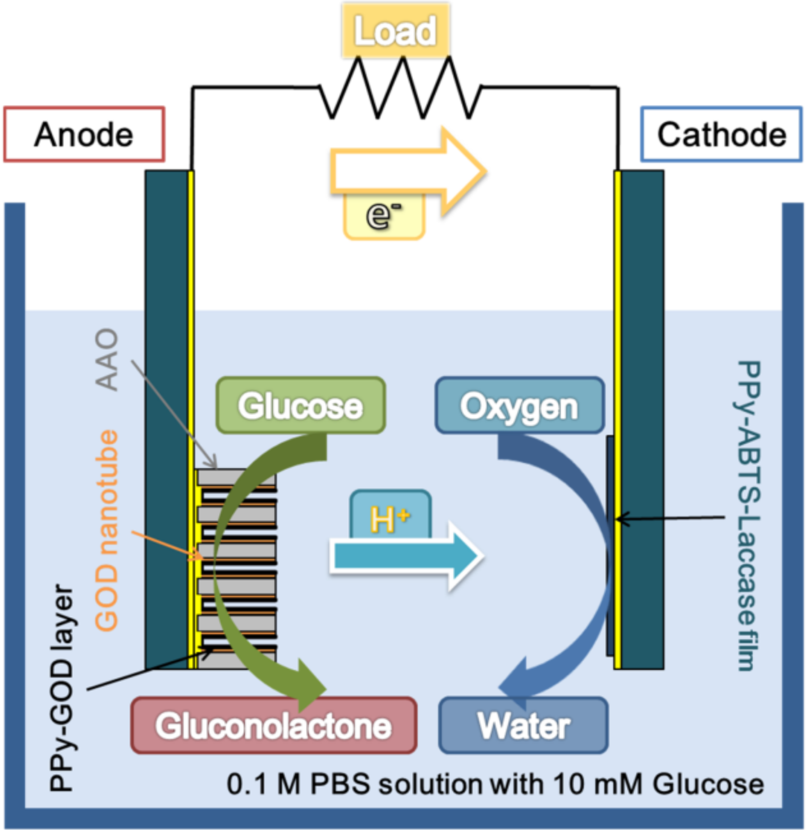

Fig. S1 Schematic illustration of glucose/O_2 biofuel cell

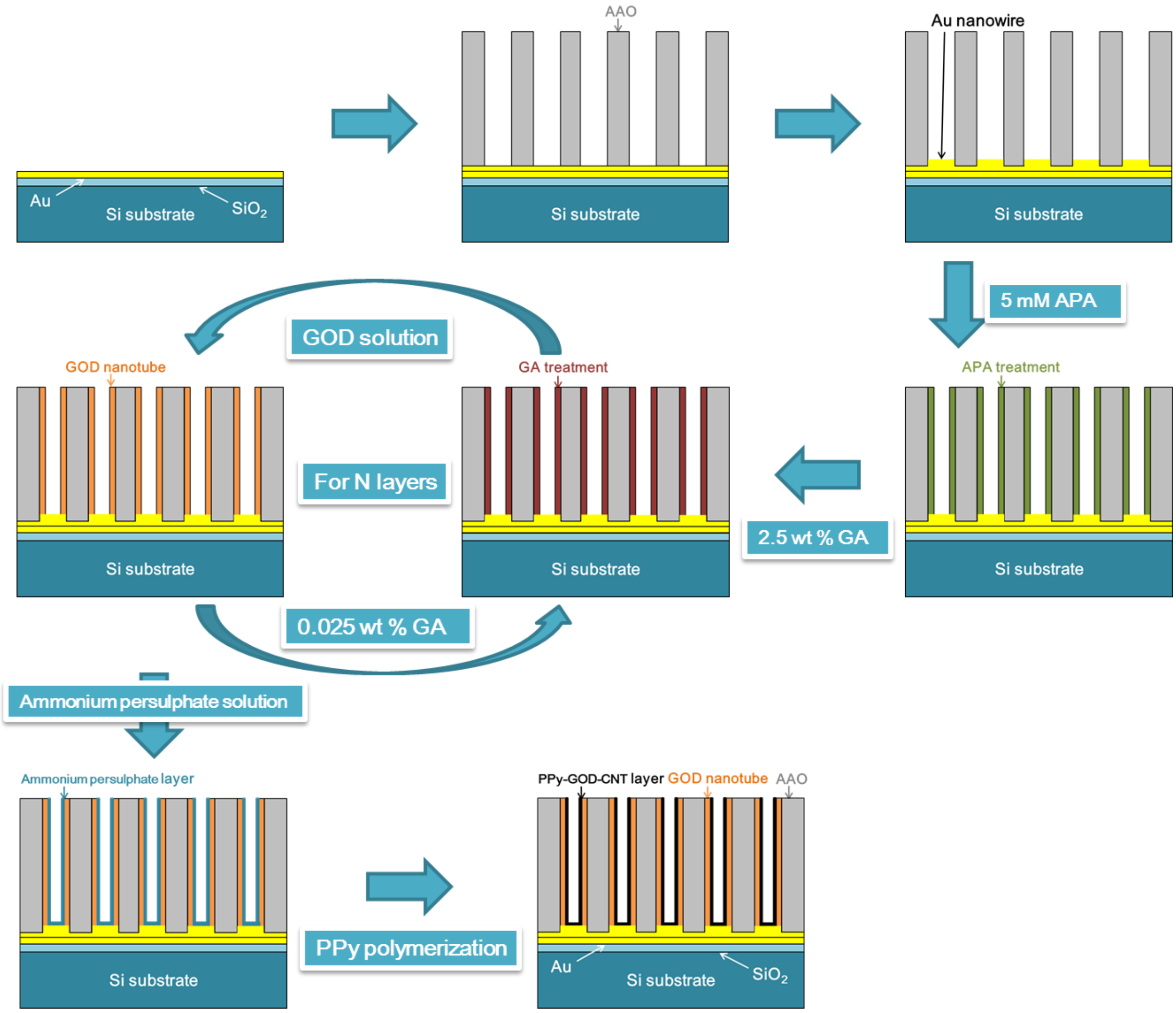

Fig. S2 The fabrication procedure of the bioanode with N layers of GOD nanotube (anode-GN-CNT)

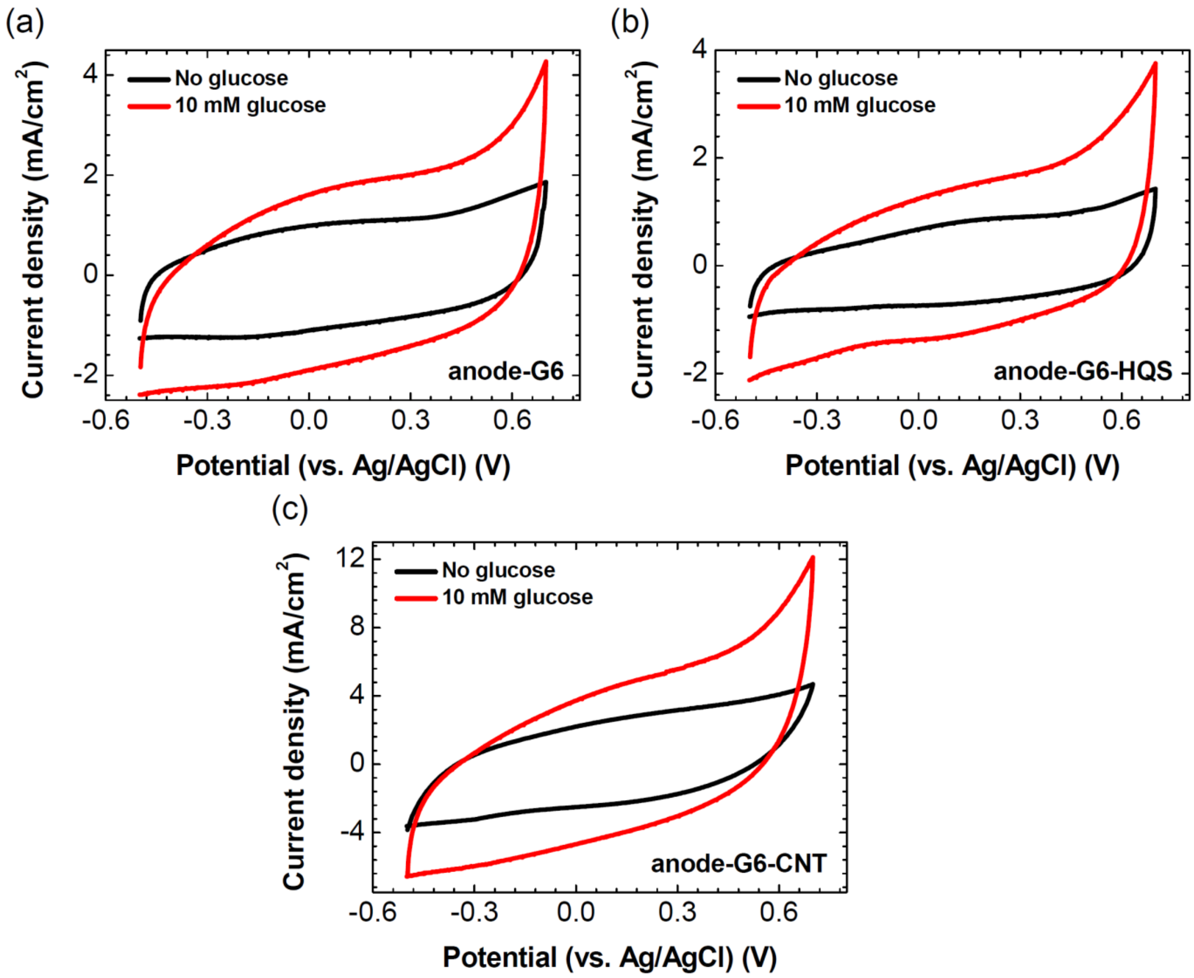

Fig. S3 Cyclic voltammograms measured in 0.1 M PBS solution, pH 7.4 with and without 10 mM glucose for (a) anode-G6, (b) anode-G6-HQS, and (c) anode-G6-CNT. Scan rate: 40 mV/s.

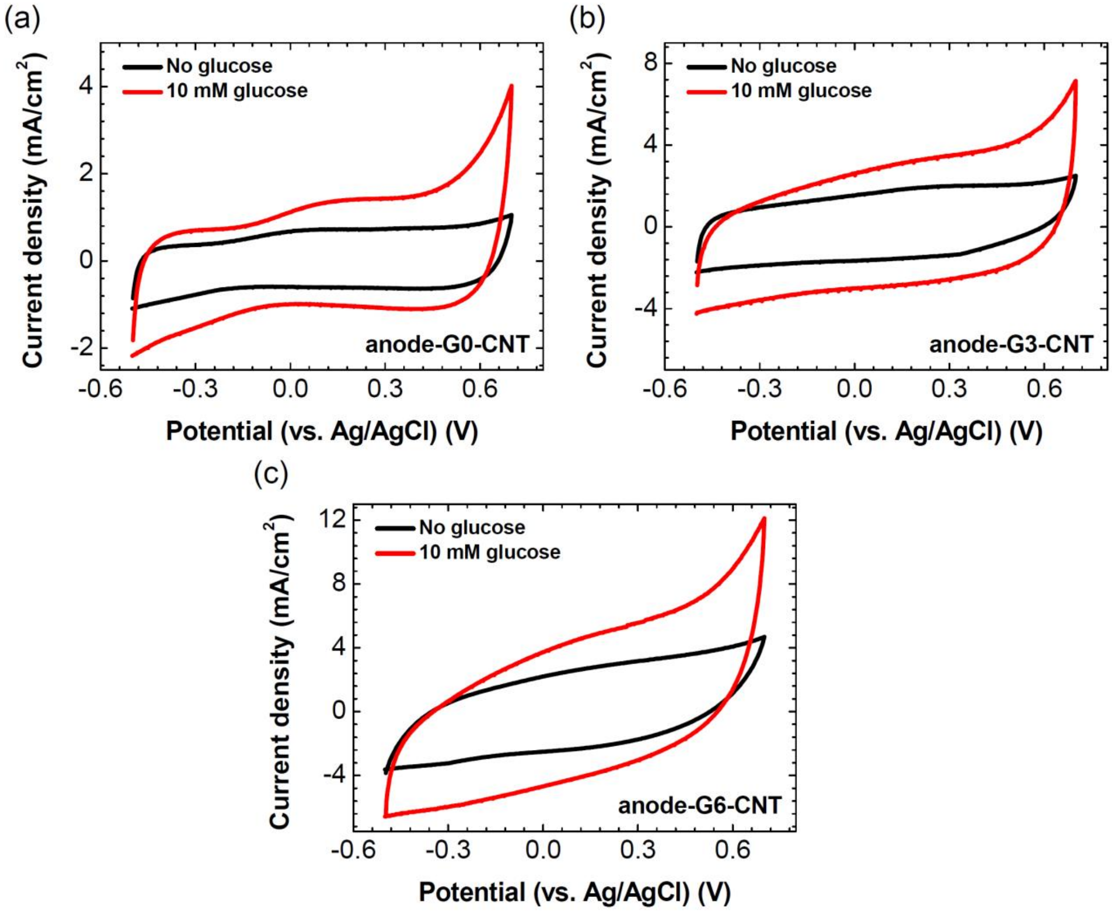

Fig. S4 Cyclic voltammograms measured in 0.1 M PBS solution, pH 7.4 with and without 10 mM glucose for (a) anode-G0-CNT, (b) anode-G3-CNT, and (c) anode-G6-CNT. Scan rate: 40 mV/s.

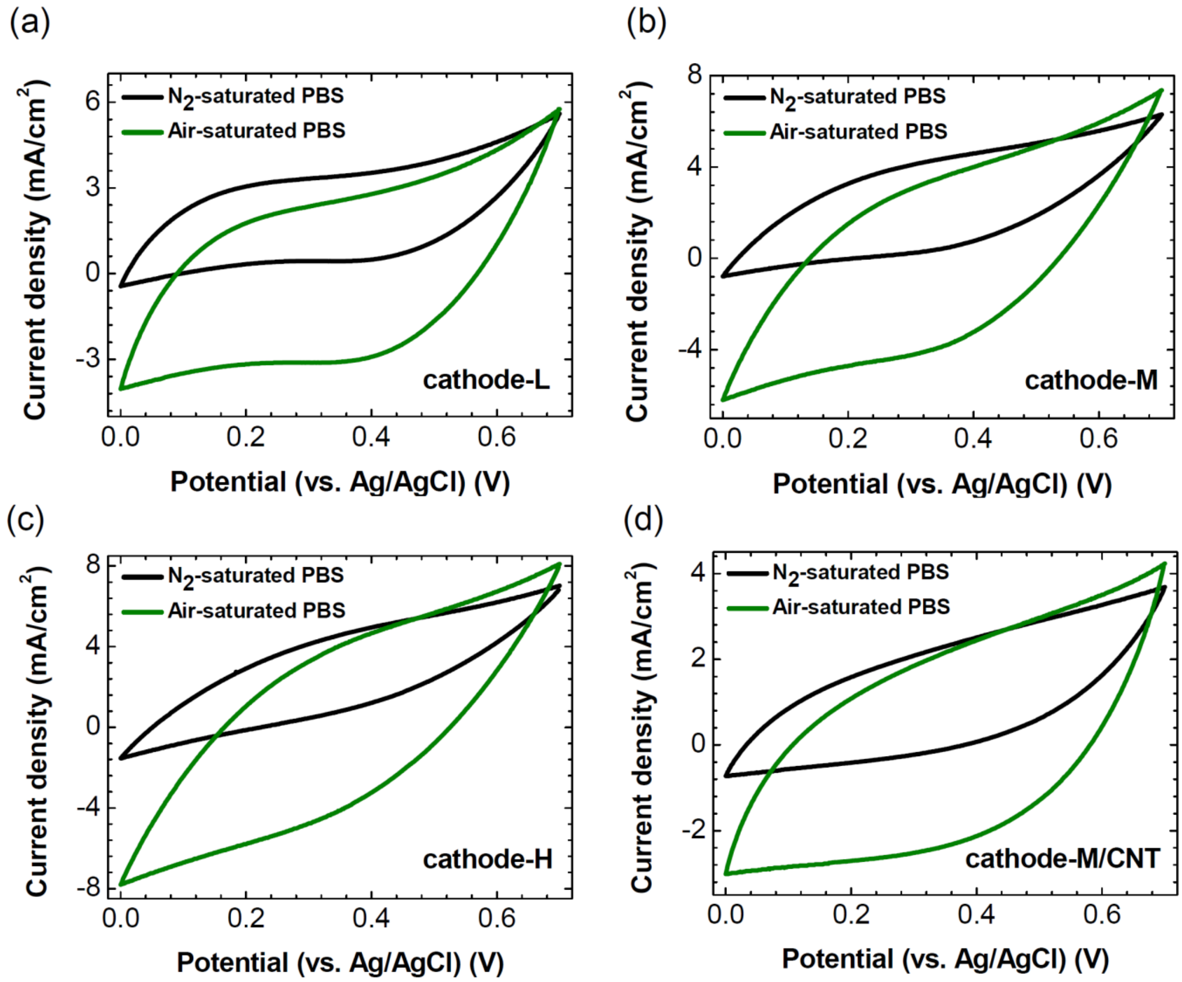

Fig. S5 Cyclic voltammograms measured in N_2-saturated and air-saturated 0.1 M PBS solution, pH 7.4 for (a) cathode-L, (b) cathode-M, (c) cathode-H, and (d) cathode-M/CNT . Scan rate: 40 mV/s.

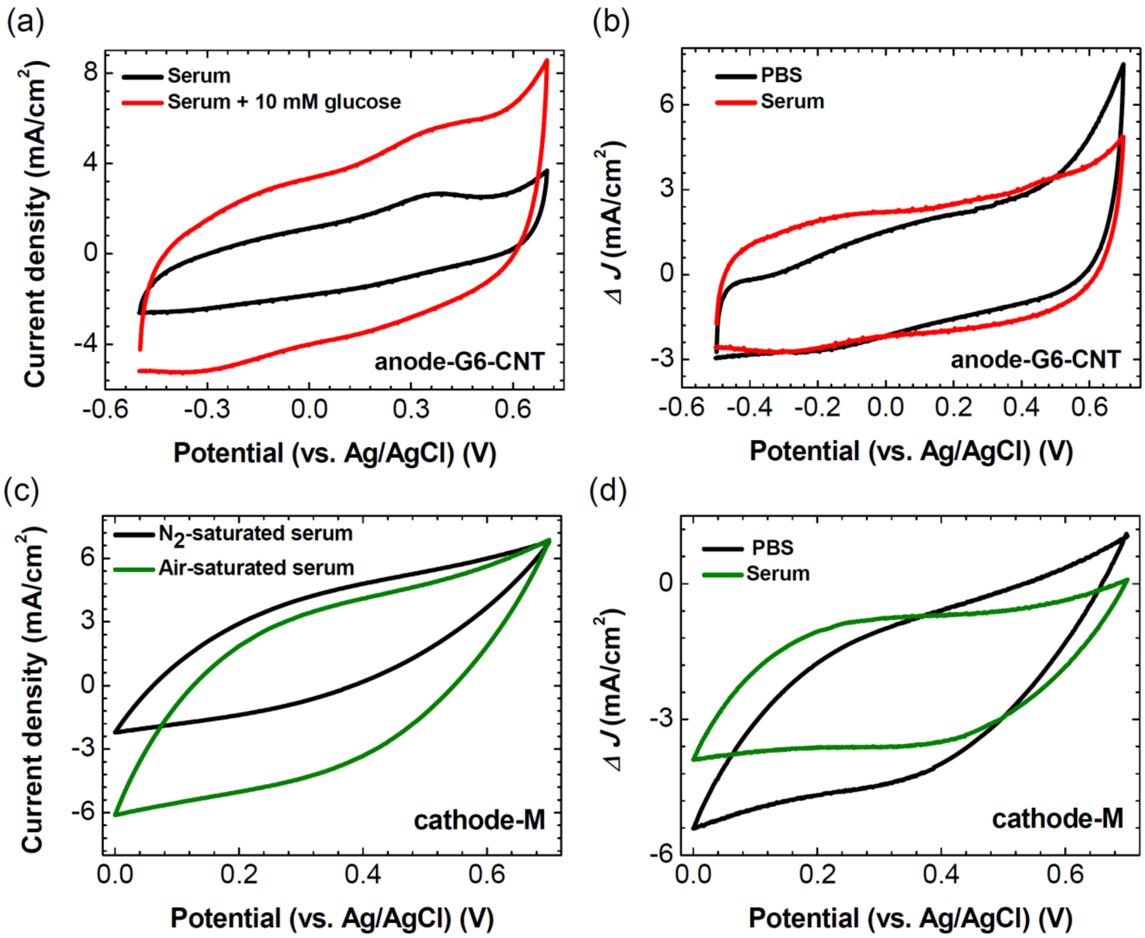

Fig. S6 (a) Cyclic voltammograms of anode-G6-CNT measured in 50 % serum with and without 10 mM glucose. (b) Background subtracted cyclic voltammograms of anode-G6-CNT in 50 % serum. ΔJ is the difference between the current densities measured in 50% serum with and without 10 mM glucose. For comparison, the plot of ΔJ versus potential in PBS is included. (c) Cyclic voltammograms of cathode-M measured in N_2-saturated and air-saturated 50 % serum. (d) Background subtracted cyclic voltammograms of cathode-M in 50 % serum. ΔJ is the difference between the current densities measured in N_2-saturated and air-saturated 50 % serum. For comparison, the plot of ΔJ versus potential in PBS is included. Scan rate: 40 mV/s.

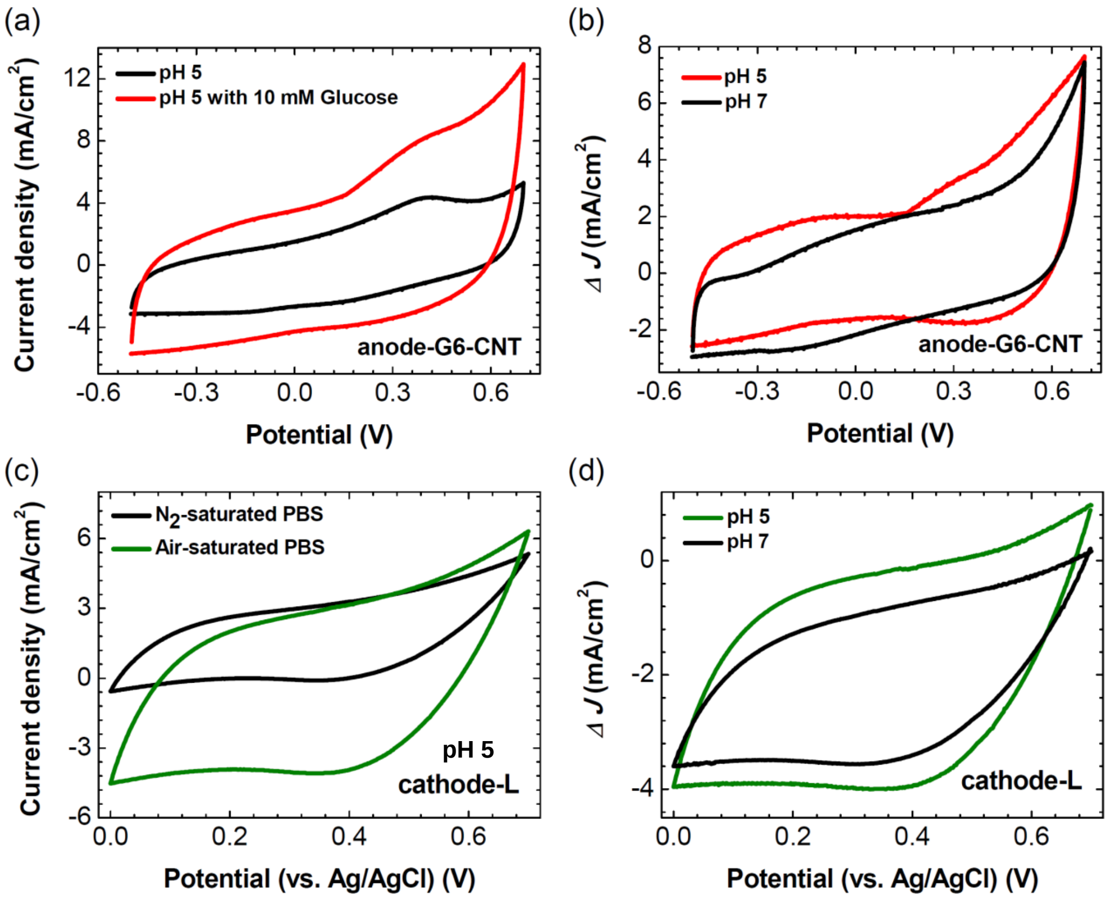

Fig. S7 (a) Cyclic voltammograms of anode-G6-CNT measured in 0.1 M PBS, pH 5 with and without 10 mM glucose. (b) Background subtracted cyclic voltammograms of anode-G6-CNT at pH 5. *ΔJ* is the difference between the current densities measured in PBS, pH 5 with and without 10 mM glucose. For comparison, the plot of *ΔJ* versus potential in PBS, pH 7.4 is included. (c) Cyclic voltammograms of cathode-L measured in N_2-saturated and air-saturated, at pH 5. (d) Background subtracted cyclic voltammograms of cathode-L at pH 5. *ΔJ* is the difference between the current densities measured in N_2-saturated and air-saturated PBS, at pH 5. For comparison, the plot of *ΔJ* versus potential at pH 7.4 is included. Scan rate: 40 mV/s.

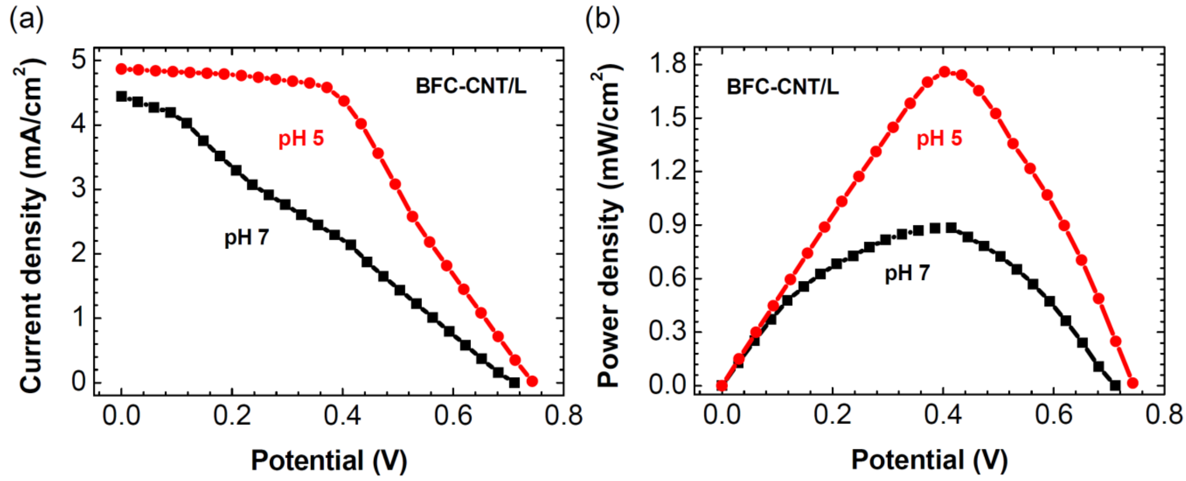

Fig. S8 Influence of pH on (a) the current density and (b) the power density of BFC-CNT/L.

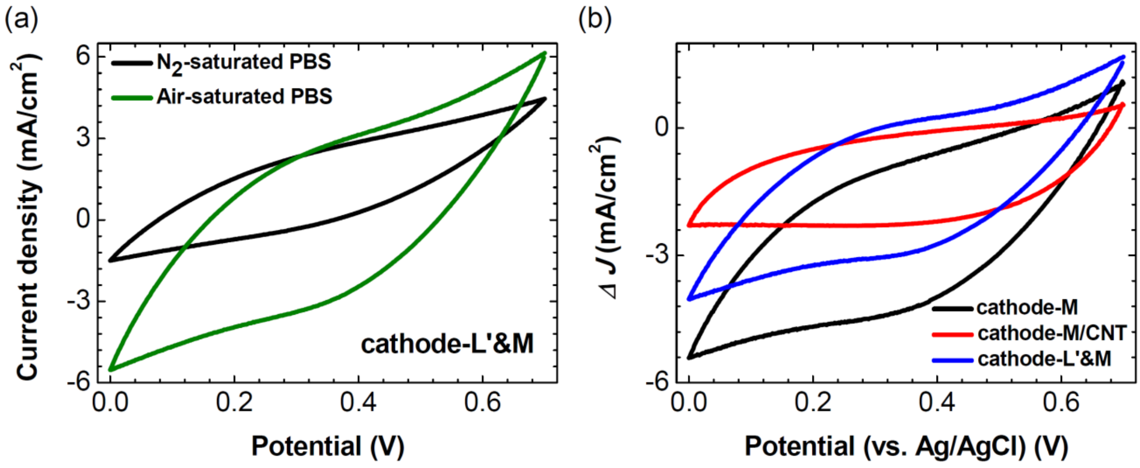

Fig. S9 (a) Cyclic voltammograms of cathode-L′&M measured in N_2-saturated and air-saturated 0.1 M PBS solution, pH 7.4. (b) Background subtracted cyclic voltammogram of cathode-L′&M. *ΔJ* is the difference between the current densities measured in N_2-saturated and air-saturated PBS. For comparison, the plots of *ΔJ* versus potential for cathode-M and cathode-M/CNT are included. Scan rate: 40 mV/s.

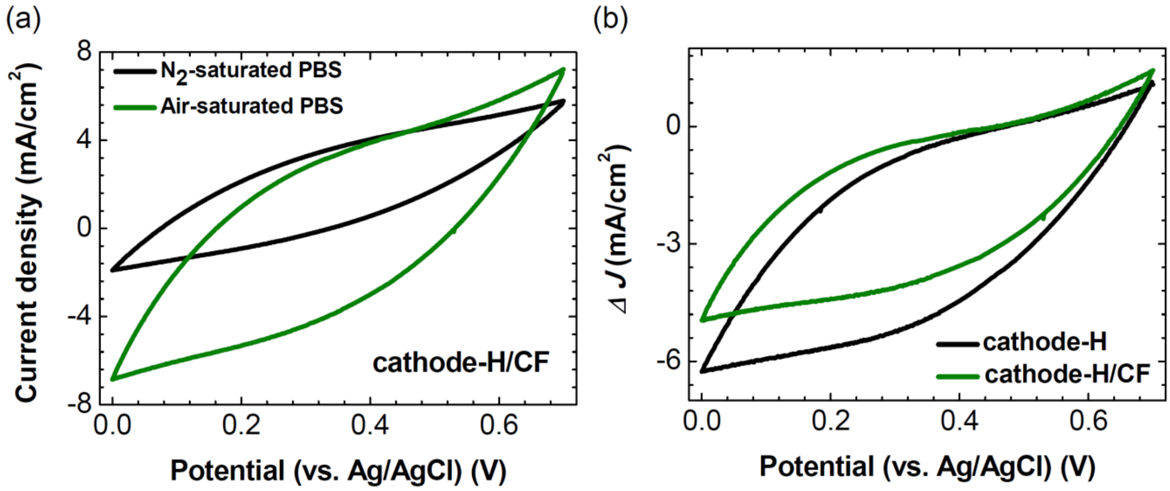

Fig. S10 (a) Cyclic voltammograms of cathode-H/CF measured in N_2-saturated and air-saturated 0.1 M PBS solution, pH 7.4. (b) Background subtracted cyclic voltammograms of cathode-H/CF. ΔJ is the difference between the current densities measured in air-saturated solution and N_2-saturated PBS. For comparison, the plot of ΔJ versus potential for cathode-H is included. Scan rate: 40 mV/s.

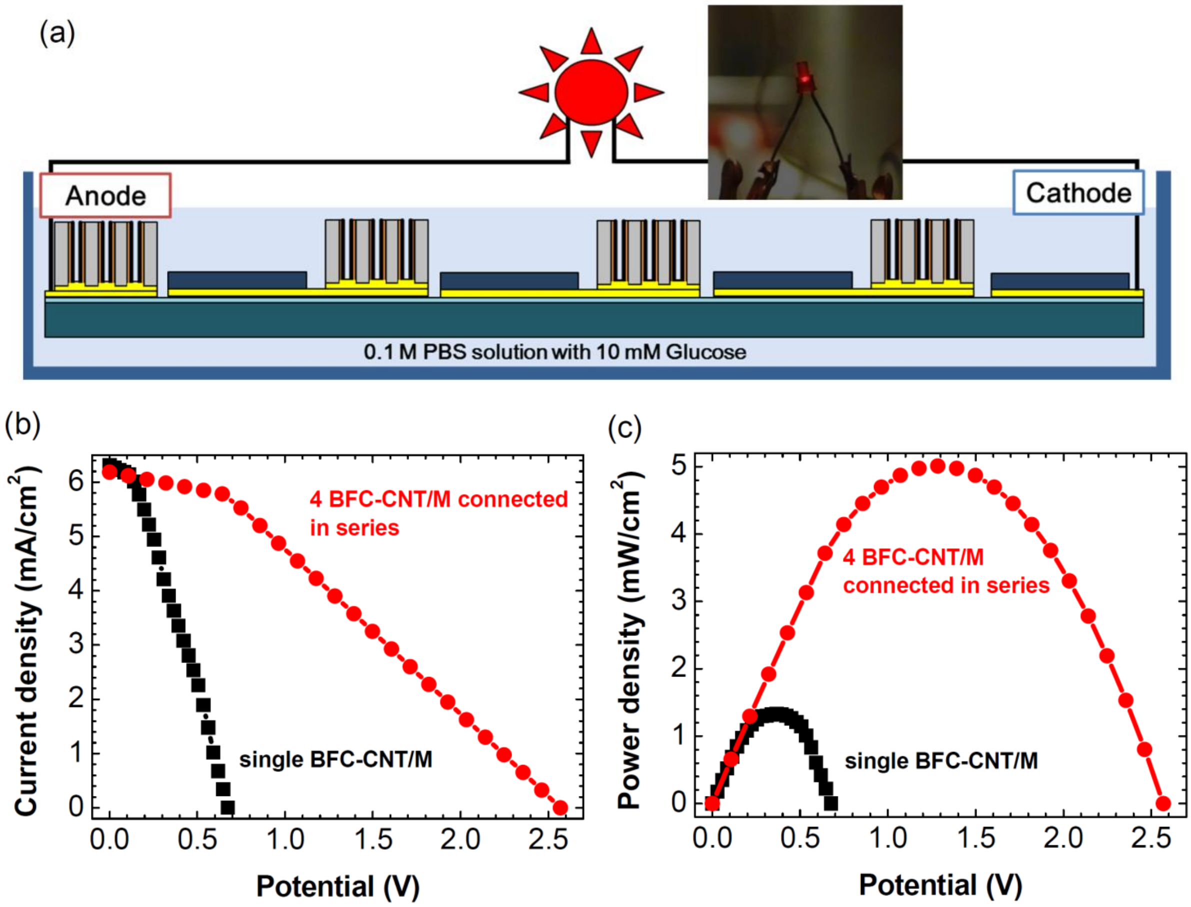

Fig. S11 (a) Schematic illustration of four BFCs connected in series in a chip with a red LED. Dependence of (b) the current density and (c) the power density on the cell voltage for BFC-CNT/M and four BFC-CNT/M which were connected in series in a chip. Measurements were performed in a 10 mM glucose solution at 37^{o}C and pH 7.4.

Table S1. Effective surface area of anode-G6-CNT and bare AAO template estimated by the Brunauer-Emmett-Teller (BET) analysis of N_2 adsorption.

	BET surface area (m^2/g)	Effective surface area for the area of 0.02 cm^2 (cm^2)
AAO/Au	9.17	17.42[(1)]
anode-G6-CNT	32.63	61.98[(2)]

[(1)] The effective surface area of bare AAO/Au was estimated using the following relationship.

$$A_{eff} = (2\pi rh+\pi r^2) \times N_{ave}$$

where r is the nanopore radius of 100 nm, h is the nanopore thickness of 60 μm, and N_{ave} is the average nanopore number of 4.03×10^7 in the area of 0.02 cm^2.

[(2)] The effective surface area of anode-G6-CNT was calculated assuming that the mass of anode-G6-CNT was almost equal to that of bare AAO/Au.

Table S2. The power density and the volumetric power for various glucose/O_2 BFCs.

Anode	Cathode	Power density (mW/cm^2)	Volumetric power (mW/cm^3)	Ref.
GOD nanotube/ PPy-GOD-CNT layers	PPy-ABTS-Laccase film	1.39	231.7	This work.
compressed MWCNT-GOD	compressed MWCNT-Laccase	1.25	1.66	(1)
GOD/HQS/PPy	Laccase/ABTS/ PPy	0.042	0.02	(2)
GOD/SWNT/PPy composite	Tyrosinase/CNPs*/PPy composite	-	0.16	(3)

*CNP is the carbon nanopowders.

1. A. Zebda, C. Gondran, A. Le Goff, M. Holzinger, P. Cinquin and S. Cosnier, *Nat. Commun.*, 2011, **2**, 370.

2. A. Habrioux, G. Merle, K. Servat, K. B. Kokoh, C. Innocent, M. Cretin and S. Tingry, *J. Electroanal. Chem.*, 2008, **622**, 97-102.

3. K. Min, J. H. Ryu, Y. J. Yoo, *Biotechnol. Bioprocess Eng.*, 2010, **15**, 371-375